Proceedings of the Australian Combustion Symposium
November 26-29, 2023, Darwin, Northern Territory

Particle residence time measurements in a flash reactor

X. Bi[1,2 *], E.W. Lewis[1,2], G.J. Nathan[1,2] and Z. Sun[1,2]
[1]Centre for Energy Technology, The University of Adelaide, SA 5005 Australia
[2]School of Electrical and Mechanical Engineering, The University of Adelaide, SA 5005 Australia

Abstract

The particle residence time distribution, $E(t)$, was measured in a lab-scale flash reactor for a pulse of particles added to a continuous jet issuing into a counter flow at room temperature. The measuring range is from the jet exit to two different downstream locations (x/d_{exit} = 62 and 124) for a series of systematically varied initial flow conditions ($\overline{U}_j/\overline{U}_c \approx 31 - 636$ for a constant $\overline{U}_c$ = 0.008 m/s and $\overline{U}_c/\overline{U}_j \approx 0.016 - 0.517$ for a constant $\overline{U}_j$ = 0.248 m/s, where $\overline{U}_j$ is the jet flow velocity and $\overline{U}_c$ is the counter flow velocity). The measurements were performed using light absorption of continuous laser beams positioned at the three aforementioned locations to allow the derivation of $E(t)$ for the two measuring ranges both starting from the exit plane. The $E(t)$ has been evaluated for the 1st and 60th percentiles, $\tau_{p,1}$ and $\tau_{p,60}$, respectively, which characterise the leading edge and the bulk flow. It was found that the characterised particle residence time has a non-monotonic relationship with the normalised jet velocity, with the values of $\overline{U}_j/\overline{U}_c$ for their ($\tau_{p,1}$ or $\tau_{p,60}$) minimum values increasing as the x/d_{exit} decreases. This is deduced to be associated with the effect of particle "group" reducing aerodynamic drag for bulk particles, while this effect can be minimised by sufficiently high jet velocity. Counter flow was found to broadly increase the particle residence time, although its effect is strong for downstream locations, while weak for the upper stream. Industrial-scale particle-based systems need to consider these different flow regimes to optimise design.

Keywords: Residence time distribution, Particle-laden flow and Flash reactor.

1. Introduction

The residence time distribution (RTD) of particles through a reactor is a critical criterion characterising the overall performance of systems, such as thermal-chemical reactions and solid mixing in fluidised beds [1, 2], microchannels [3], solar particle reactors [4] and flash reactors [5]. The RTD of particles has been introduced to describe the probability function of the residence time of particles within a region of interest and operating conditions. However, this function is challenge to measure because it cannot be derived directly from local measurements of velocity and because of the challenges of performing any in-situ measurements in high temperature industrial reactors. The processes within them are complex, involving multi-mode heat and mass transfer that is non-linearly coupled with particle and fluid dynamics, and an inaccessible environment for most of the available measuring techniques [6]. Therefore, there is currently a lack of reliable measurements providing data for such systems, in turn inhibiting the processes of optimisation, upscaling and design. The overall aim of this work is to meet this need through developing and applying a method to reliably measure RTD within an industrially relevant, lab-scale reactor.

Flash reactors employing particle-laden flows are widely used in industry for high temperature processes such as ironmaking, alumina and cement calcination [7-9]. One type of these reactors consists of a vertical chamber with a set of inlets at the top to feed raw material, through which particles fall under the influence of gravity, and outlets at the base to collect processed product. The simplicity of this device also makes it relevant to model validation, and hence will also support the development of other types of more complex reactor.

The challenges of measuring RTD in particle flow reactors have led to previous measurements. Early work was typically performed using different types of tracers [1]. Despite the usefulness of this method in providing data of relevance to particles that are sufficiently small to approach perfect flow tracers or identical to main particles in the flow, it is unable to account for two-phase effects. More recently, Davis *et al.* [4] developed a method in which a small burst of particles was introduced into a steady-flowing gas stream as both the tracer and the medium being traced. This is an important development in that it accounts for two-phase flow effects, albeit it being limited to dilute phase regime. Nevertheless, those measurements were limited to inflow and outflow through a swirling reactor, so there is a need to extend this to provide better understanding of in-situ distributions through jet-like flow reactors, whose flow-fields are better understood.

To meet this need, the present investigation aims to improve understanding the RTD of particles through a well characterised, lab-scale jet-flow environment that is both directly relevant to a particular class of flash reactor and also well suited to the development and validation of numerical models. This is performed for a systematically varied series of particle inlet and internal reactor flows.

2. Experimental Approach

Figure 1 presents the experimental arrangement used to allow optical measurement of the RTD of the pulse of particles through a lab-scale flash reactor at room temperature. The reactor body is a vertically-aligned acrylic pipe with inner diameter d_{pipe} = 190 mm, with a coaxial stainless-steel pipe jet of exit diameter d_{exit} = 10.2 mm used to feed particles from the top of the system. Particles were released into a continuous flow of carrier

* Corresponding author: Xiaopeng Bi

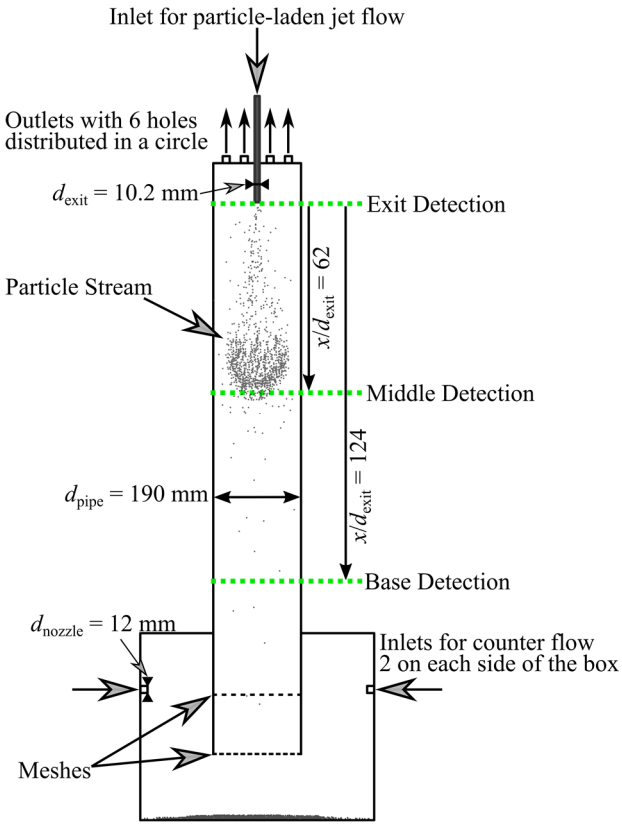

Figure 1. Experimental arrangement with three levels of optical detection to determine the particle residence time distribution for a pulse particle-laden jet flow in a lab-scale flash reactor. The particle flow is injected with compressed air from a top central tube, while a counter flow is supplied and evenly distributed by eight nozzles symmetrically positioned at each side of the cubic wall of a bottom box.

air via a ball valve, to generate a pulse of particles within a continuous jet. The particles issue downward to an upward (counter) flow of air supplied from eight nozzles (d_{nozzle} = 12 mm) evenly distributed on the side walls of a plenum, which also doubles as the particle collection box. Two mesh screens were used at the bottom section of the rig with eight mesh cups covering the inlets of the counter flow to generate a spatially uniform counter flow within the system. Separate mass flow controllers were

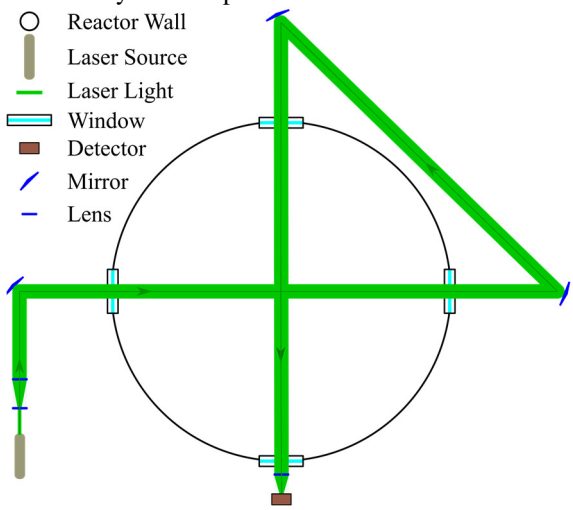

Figure 2. Optical arrangement detecting particle signals for deriving particle residence time distribution. The laser beam is arranged to cross the reactor centerline twice to detect the bulk flow of dispersed particles. Note that the exit detection channel only consists of a single beam as it is sufficiently large to cover the jet exit.

used to control the flow rates through the jet and counter flow, to provide bulk velocities in the range 0.248 m/s ≤ $\bar{U}_j$ ≤ 5.101 m/s and 0.008 m/s ≤ $\bar{U}_c$ ≤ 0.128 m/s, respectively. PMMA particles (microbeads spheromers) with density of 1200 kg/m^3, particle diameter $\bar{d}_p$= 80 µm and bulk volume of 0.5 mL were used for each pulse of particles.

Figure 2 presents the optical arrangement used to transmit the laser through each of the measurement planes to detect the passage of the pulse of particles. These were arranged at the three downstream distances (x) from the jet exit plane, x/d_{exit} = 0, 62 (middle) and 124 (base). All of the optical parts were mounted to an external aluminium frame around the main rig.

A continuous 532 nm laser beam (Thorlabs CP5532), with a beam power of ~ 4.5mW was expanded to provide a collimated beam of ~ 20 mm diameter. This laser beam was double crossed at the centre of the reactor by a series of optical mirrors to extend the beam path length used for particle signal detection. At the end of the beam path, a light detector (DET100A2) was used to continuously detect the intensity of the laser light beam during the measurement. Note that this arrangement of double laser beam was only applied to the middle and base detection channels, while the exit detection used a single laser beam, with all the other settings same as the double beam arrangement. This is because the cross-sectional area of a single beam is sufficiently large to detect the whole exit of the particle discharge tube.

The RTD of particles was derived using the well-known convolution-deconvolution method [4, 6, 10, 11]. This method assumes the outlet concentration of particles is the result of convolution of the inlet particle concentration with the particle RTD within this section. The equation is given as follows,

$$o(t) = i(t) * E(t) = \int_0^t i(t-t')E(t')dt', \qquad (1)$$

where, i(t) and $o(t)$ are the inlet and outlet particle concentration as a function a time for a certain study region, and $E(t)$ is the RTD of particles within a reactor. A fast Fourier transform was performed on the measured particle signals that are intensity-based particle concentration to derive the $E(t)$ for the distance between detection channels, i.e., x/d_{exit} = 0 ~ 62 and 0 ~ 124.

3. Results and Discussion

Figure 3 presents a typical measurement of the temporal profile of particle signal distribution, normalised by area, calculated from the light extinction measurement for the flow with $\bar{U}_j$ = 1 m/s and $\bar{U}_c$ = 0.008 m/s. A narrow temporal distribution can be identified for the exit (0 ~ 1 s), while it spreads for the base (1.1 s ~ 6.7 s). This indicates that the initial particle pulse disperses gradually through the system.

It can be also seen from Fig. 3 that the detected particle signals are highly skewed, with a rapid rise followed by a lower decay rate (the tail). This is because the leading-edge particles are densely laden due to the high initial volume fraction when the pulse is introduced and the high

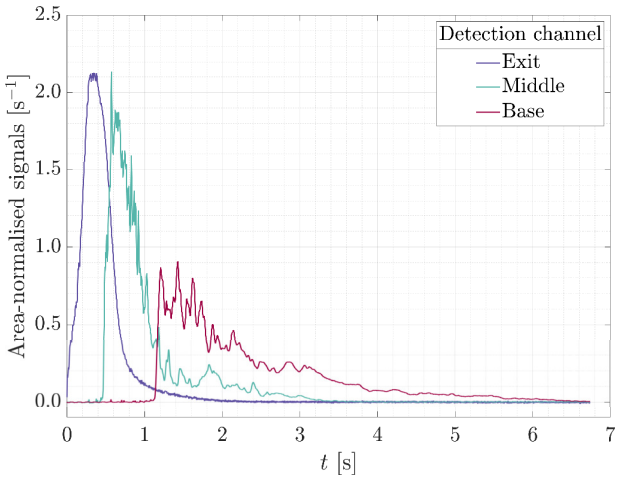

Figure 3. Measured particle signals in the time domain for three levels of detection. Here, $\bar{d}_p$ = 80 µm, $\overline{U}_j$ = 1 m/s, $\overline{U}_c$ = 0.008 m/s.

gradient in number density, followed by a long wake. This non-linear phenomenon has been explained with a detailed force balance in a study of free-falling particle flows [12], that include the formation of a particle "group" at the front where drag mainly acts on the exterior side due to the short particle-particle distance within the bulk particles, and a discrete particle "tail" due to turbulent wake (see Fig. 1). The difference in the decay and rising rate of particle signal becomes more significant with downstream distance as a result of the integration of these effects with time and distance.

Figure 4 presents the particle residence time distribution $E(t)$ that is derived using the convolution-deconvolution method in Eq. (1). These are consistent with their corresponding area-normalised particle signals. This implies that the temporal profile of particle signal at the exit level from a near-perfect plug flow (Fig. 3), has only a small effect on the profile of $E(t)$. The sharp rise of the $E(t)$ indicates that the peak concentration occurs ~ 0.1 s after the leading edge of particles, with trailing particles passing up to ~ 3 s later.

Figure 5 presents statistical measures of the cumulative $E(t)$ including $\tau_{p,1}$ and $\tau_{p,60}$ as a function of a series of normalised $\overline{U}_j$ and $\overline{U}_c$ for x/d_{exit} = 62 and 124.

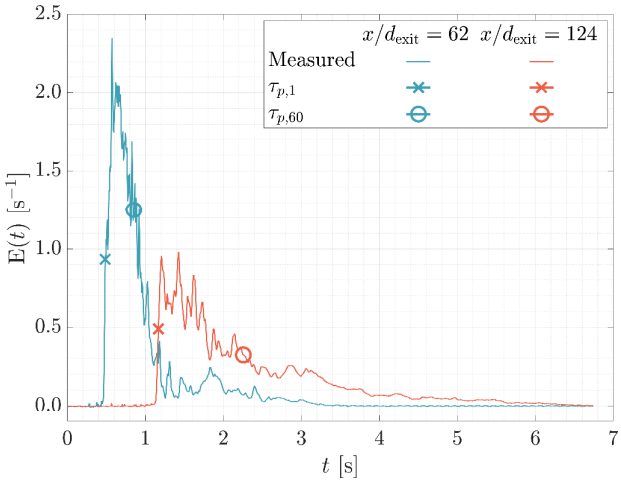

Figure 4. Particle residence time probability distribution, $E(t)$, from the jet exit to x/d_{exit} = 62 and 124 with markers identifying the 1% and 60% cumulative $E(t)$, denoted by $\tau_{p,1}$ and $\tau_{p,60}$, respectively. Here, $\bar{d}_p$ = 80 µm, $\overline{U}_j$ = 1 m/s, $\overline{U}_c$ = 0.008 m/s.

These corresponding to 1% and 60% values of the cumulative $E(t)$ function, namely $\tau_{p,1}$ and $\tau_{p,60}$, defined as $\int_0^{\tau_{p,1}} E(t)dt = 0.01$ and $\int_0^{\tau_{p,60}} E(t)dt = 0.6$, respectively. Both $\tau_{p,1}$ and $\tau_{p,60}$ at x/d_{exit} = 124 are greater than twice that of x/d_{exit} = 62 for all subfigures, demonstrating that the particles generally decelerate between the two falling distances. This is because particle-air interaction is expected to increase with downstream distance as particles continuously disperse, reducing the "group" effect, while the axial counter flow distribution is relatively uniform, impeding the particle fall. The error bar based on one standard deviation calculated from five repetitions is shown. This provides confidence in the repeatability of the measurement.

Figure 5 (a) presents a plot of the dependence of that $\tau_{p,1}$ and that $\tau_{p,60}$ on the velocity ratio of jet to counter flow $\overline{U}_j/\overline{U}_c$ at two downstream locations. It can be seen that $\tau_{p,1}$ for x/d_{exit} = 62 decreases monotonically with an increase in $\overline{U}_j$ as expected because an increase in initial velocity will reduce the time needed for particles to move through the pipe. However, further downstream at x/d_{exit} = 124, the trend is non-monotonic. After the initial decrease from $\tau_{p,1}$ = 2.36 s to 1.13 s for $\overline{U}_j$ = 0.248 m/s and 1.996 m/s, respectively, $\tau_{p,1}$ then increases for $\overline{U}_j$ = 3.5 m/s and 5.1 m/s to $\tau_{p,1}$ = 1.32 s and 1.76 s. A plausible explanation is that velocity is sufficient to cause a decrease in the aforementioned particle "group" effect, thereby inducing greater particle-air interaction, increasing the $\tau_{p,1}$. This phenomenon can be also observed for $\tau_{p,60}$ for both falling ranges. While the trends in all data sets are broadly consistent, the value of $\overline{U}_j/\overline{U}_c$ for the minimum defined particle residence time can be seen to increase with the decrease in distance, and may even be beyond the range of present data for the $\tau_{p,1}$ at x/d_{exit} = 62. That is, for this case, the value of $\overline{U}_j/\overline{U}_c$ for the minimum $\tau_{p,1}$ may locate outside the current scope of the velocity ratio, potentially indicating a strong particle "group" effect for particles that $\tau_{p,1}$ characterises. This is consistent with $\tau_{p,1}$ characterises the leading edge of the pulse of particles, whilst $\tau_{p,60}$ characterises the bulk flow behaviour. However, more data is needed to better understand these effects, particularly the influence of all of these parameters on the particle "group".

Figure 5 (b) shows that the counter flow extended the particle residence time at all studied falling distances, as expected. This is because the counter flow generates upwards air momentum impeding particle fall. For x/d_{exit} = 124, $\tau_{p,60}$ can be increased by 140% when $\overline{U}_c/\overline{U}_j$ is increased from 0.016 to 0.517. This effect is only weak for $\tau_{p,1}$ of x/d_{exit} = 62, plausibly due to the top section is still in the jet momentum influential region and particles at the leading edge in this region are self-dominated by particle momentum.

4. Conclusions

New insights of the effects of the jet flow and counter flow on the particle residence time of a pulse particle flow

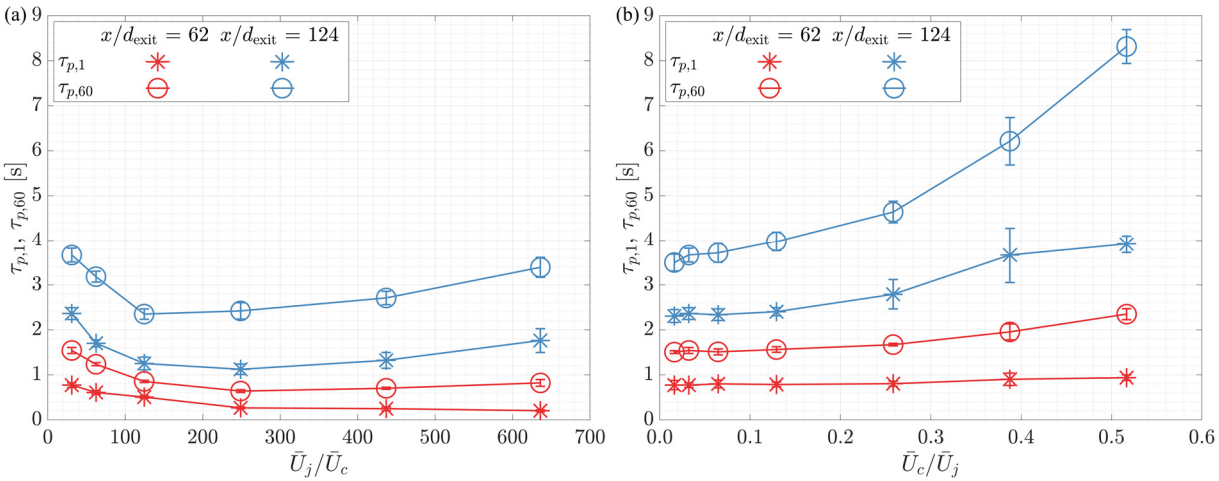

Figure 5. The statistical measures of particle residence time for x ranges of 0 - 0.63 m and 0 - 1.26 m under different flow conditions. The influence of normalized jet flow velocity on 1% and 60% cumulative $E(t)$ is presented in (a) with a constant $\bar{U}_c$ = 0.008 m/s, while (b) shows the effect of normalized counter flow velocity on them with a constant $\bar{U}_j$ = 0.248 m/s. Particle diameter is kept constant with $\bar{d}_p$ = 80 µm.

between particle exit to two different downstream locations (x/d_{exit} = 62 and 124) in a confined lab-scale flash reactor have been provided. The $\tau_{p,60}$ (characterise the bulk particle flow) of x/d_{exit} = 62 and 124, and $\tau_{p,1}$ (characterise the leading-edge particles) of x/d_{exit} = 124 were found to be non-monotonically dependent on the normalised jet velocity with the values of $\bar{U}_j/\bar{U}_c$ for their ($\tau_{p,1}$ or $\tau_{p,60}$) minimum values increasing as the x/d_{exit} decreases. The $\tau_{p,1}$ of x/d_{exit} = 62 was found to be monotonically dependent on the $\bar{U}_j/\bar{U}_c$ possibly because the jet velocity used in the present study was not sufficient to break their "group" effect, which is deduced to be responsible for the trend of the characterised particle residence time. However, more work is needed to better understand and confirm the controlling influences. Counter flow was found to broadly increase the particle residence time, although its effect is strong for downstream locations, while weak for the upper stream. For other industrial systems employing particle flows, this work suggests a direct in-situ measurement of flow field is important for understanding the efficacy of relevant parameters in engineering processes.

5. References

[1] A. Harris, J. Davidson and R. Thorpe, Chem. Eng. Sci. 58 (11) (2003) 2181-2202.

[2] K. Chen, P. Bachmann, A. Bück, M. Jacob and E. Tsotsas, Powder Technol. 345 (2019) 129-139.

[3] S. Chen, Q. Lin, N. Pan, M. Hao, Y. Jiang, Y. Xie, Y. Ba, X. Bian and K. Liu, Phys. Fluids 35 (8) (2023).

[4] D. Davis, M. Troiano, A. Chinnici, W.L. Saw, T. Lau, R. Solimene, P. Salatino and G.J. Nathan, Chem. Eng. Sci. 214 (2020) 115421.

[5] S. Xiu, Z. Li, B. Li, W. Yi and X. Bai, Fuel 85 (5-6) (2006) 664-670.

[6] P.V. Danckwerts, Chem. Eng. Sci. 50 (24) (1995) 3857-3866.

[7] F. Chen, Y. Mohassab, T. Jiang and H.Y. Sohn, Metall. Mater. Trans. B 46 (1) (2015) 1133-1145.

[8] J.R. Fernandez, S. Turrado and J.C. Abanades, Reaction Chemistry & Engineering 4 (12) (2019) 2129-2140.

[9] A. Kontopoulos, K. Krallis, E. Koukourakis, N. Denaxas, N. Kostis, A. Broussaud and O. Guyot, Appl. Therm. Eng. 17 (8-10) (1997) 935-945.

[10] Y. Gao, F.J. Muzzio and M.G. Ierapetritou, Powder Technol. 228 (2012) 416-423.

[11] A.H. Essadki, B. Gourich, C. Vial and H. Delmas, Chem. Eng. Sci. 66 (14) (2011) 3125-3132.

[12] Y. Wang, X. Ren, J. Zhao, Z. Chu, Y. Cao, Y. Yang, M. Duan, H. Fan and X. Qu, Powder Technol. 292 (2016) 14-22.